Supporting Information

for

Dual Targeting Antibacterial Peptide Inhibitor of Early Lipid A Biosynthesis

Ronald J. Jenkins and Garry D. Dotson

Department of Medicinal Chemistry, College of Pharmacy

University of Michigan, Ann Arbor, MI 48109

Email: gdotson@umich.edu

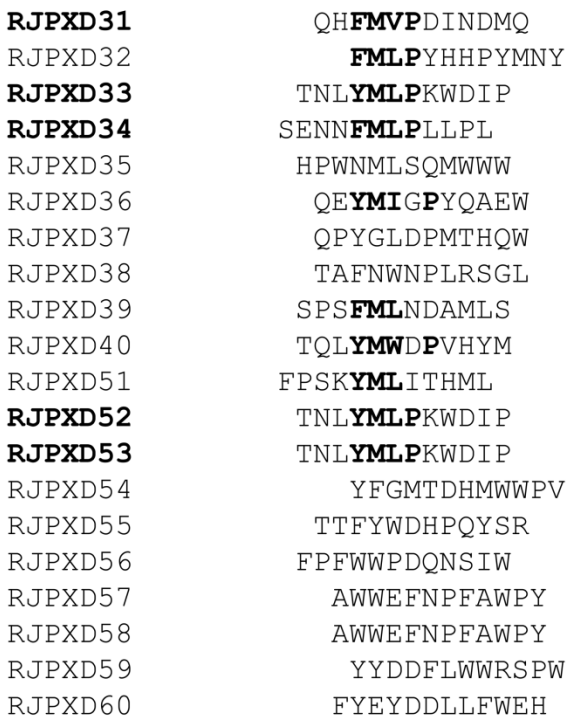

Figure S1. Multiple sequence alignment of dodecapeptides identified from competition phage display experiments. Twenty sequences were aligned using Clustal W **(*1*)**. Peptides highlighted in bold showed antibacterial activity upon expression in *E. coli* XL1 Blue. Amino acids highlighted in bold reveal a consensus motif (Y/FMLP) identified within many of the peptides. RJPXD33 was identified among three of the twenty randomly selected colonies, representing 15% of total colonies selected.

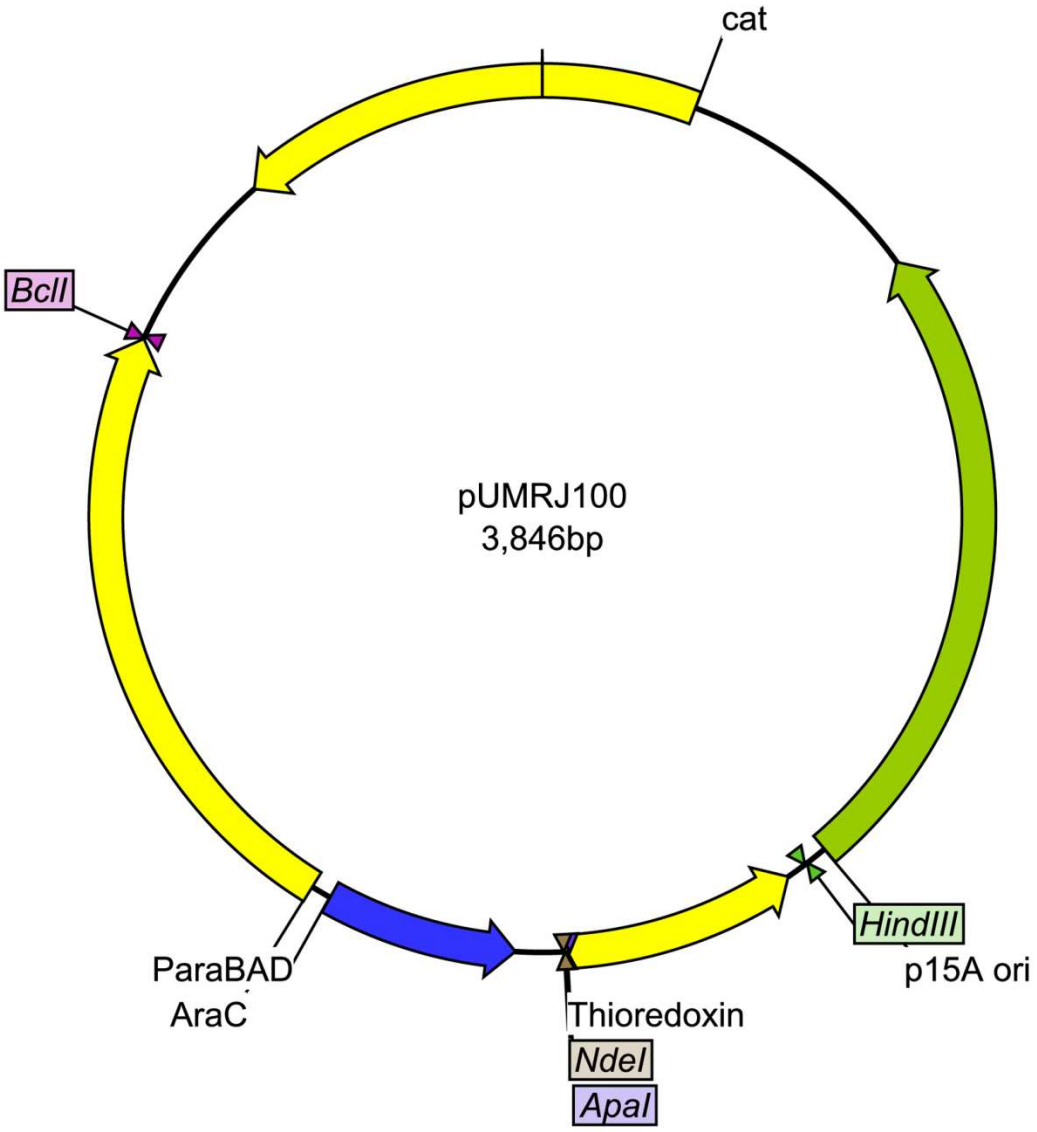

Figure S2. Bioactivity screening plasmid. Peptide coding sequences identified from phage display were cloned separately into the *NdeI*/*ApaI* sites of pUMRJ100. Upon induction with L-arabinose in *E. coli* XL1 Blue the cloned peptides are expressed as protein fusions with thioredoxin.

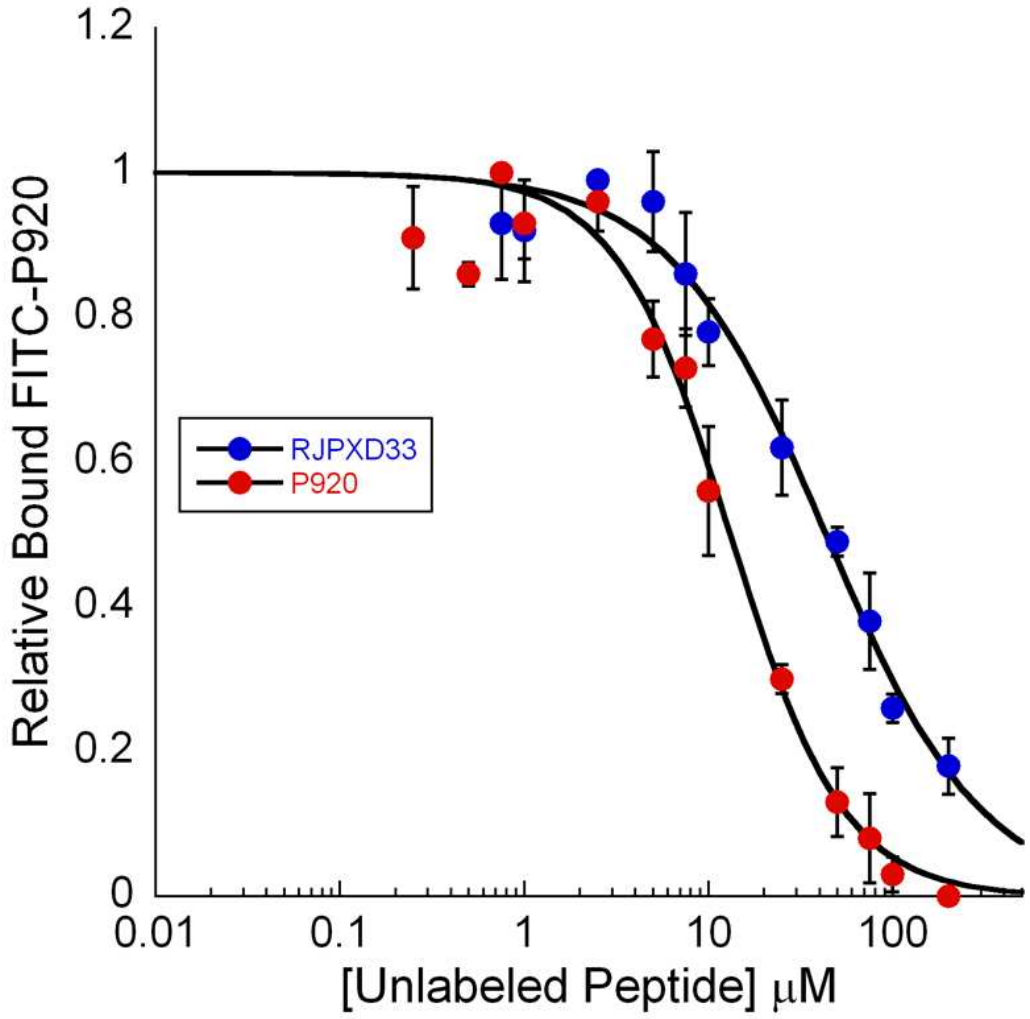

Figure S3. Competetion binding data for RJPXD33 and P920 binding to LpxA. A fluorescent, competition LpxA binding assay, in which FITC-P920 (20 nM) and LpxA (220 nM) were held constant while unlabeled competing peptide (RJPXD33 (blue) or P920 (red)) was titrated at various concentrations. In addition to binding to LpxD, unlabeled RJPXD33 was able to compete with FITC-920 for binding to LpxA. Data points represent the mean of three individual experiments while error bars represent the standard deviation. The relative amount of bound labeled peptide was normalized by dividing the ΔmP obtained in the presence of competing peptide by the ΔmP obtained in the absence of competing peptide.

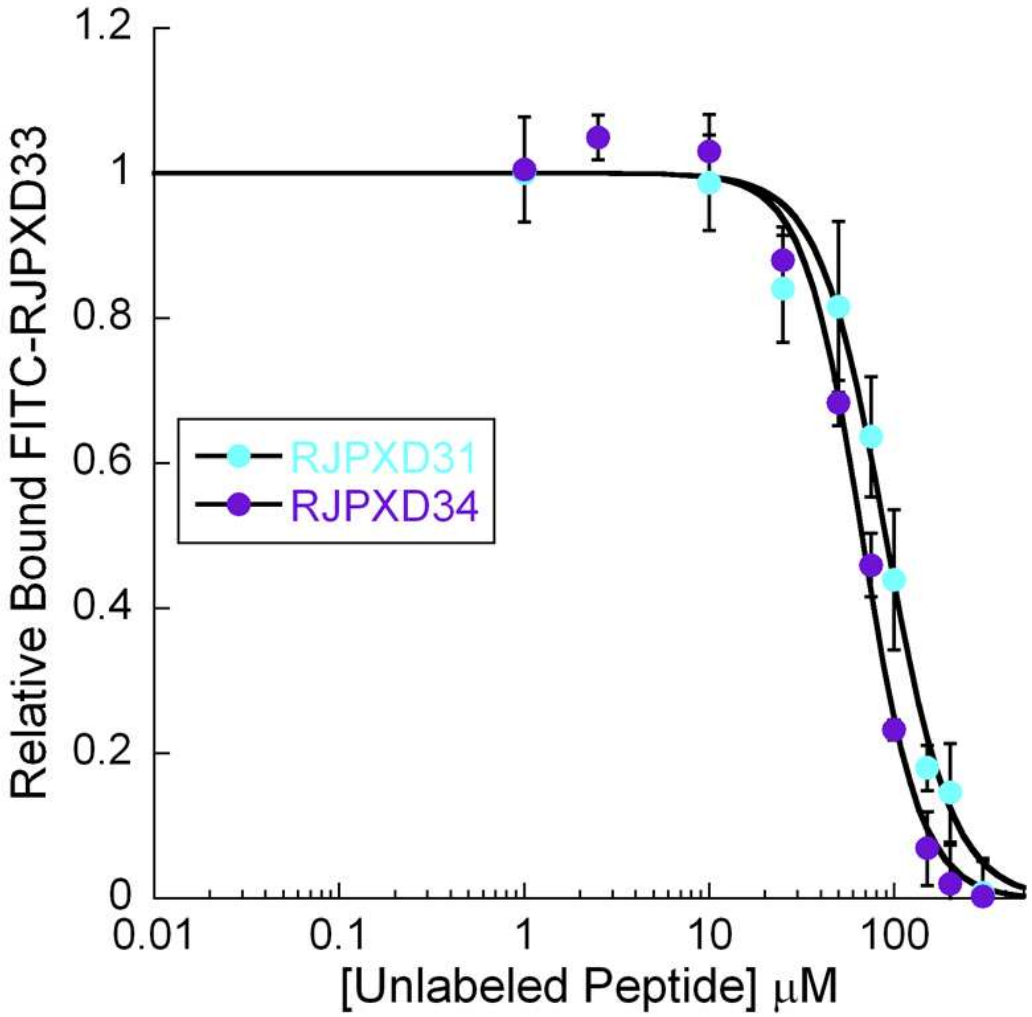

Figure S4. Competetion binding data for RJPXD31 and RJPXD34 binding to LpxD. FITC-RJPXD33 (20 nM) and LpxD (660 nM) were held constant while RJPXD31 and RJPXD34 were titrated at increasing concentrations. Both peptides where able to displace labeled peptide bound to LpxD. Data points represent the mean of three individual experiments while error bars represent the standard deviation. The relative amount of bound labeled peptide was normalized by dividing the ΔmP obtained in the presence of competing peptide by the ΔmP obtained in the absence of competing peptide.

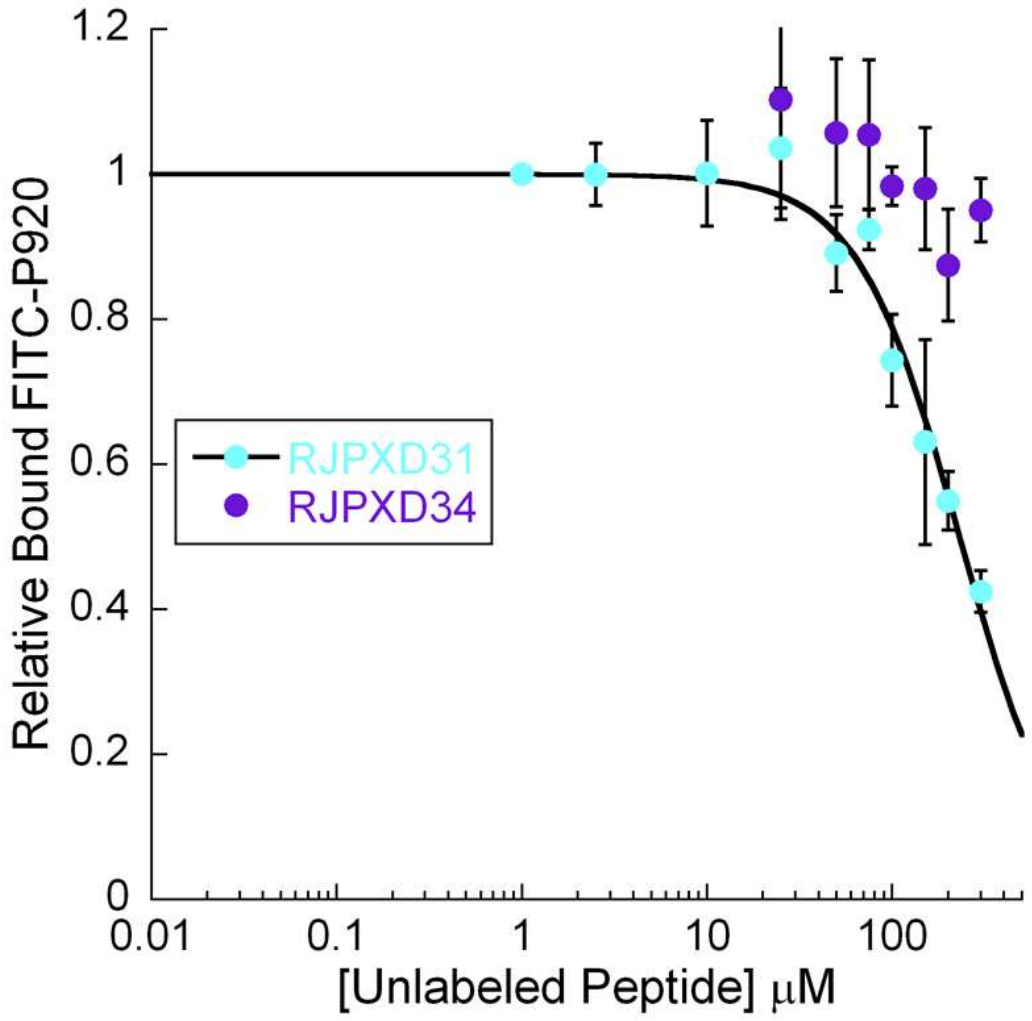

Figure S5. Competetion binding data for RJPXD31 and RJPXD34 binding to LpxA. FITC-P920 (20 nM) and LpxA (220 nM) were held constant while increasing concentrations of unlabeled RJPXD31 (cyan) and RJPXD34 (purple) were titrated. RJPXD34 did not show significant binding to LpxA at concentrations up to 300 μM. Data points represent the mean of three individual experiments while error bars represent the standard deviation. The relative amount of bound labeled peptide was normalized by dividing the ΔmP obtained in the presence of competing peptide by the ΔmP obtained in the absence of competing peptide.

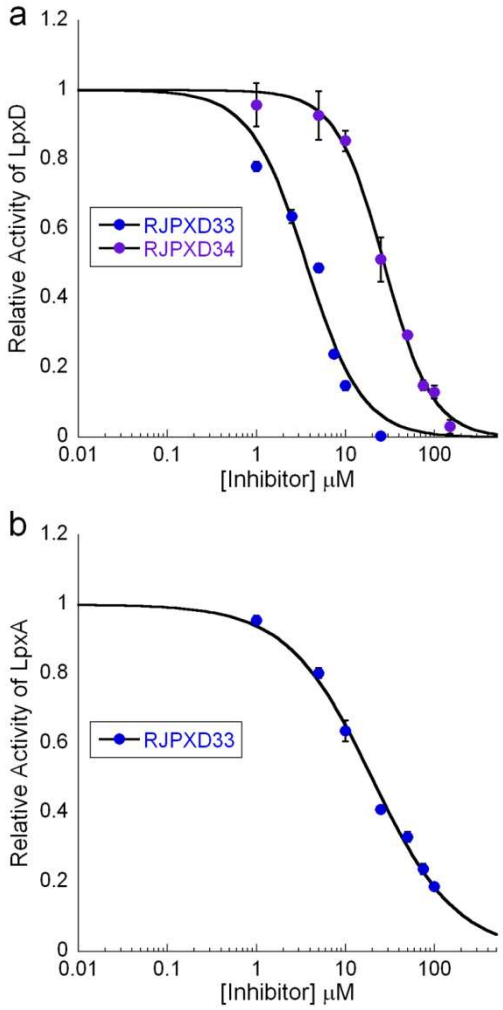

Figure S6. IC50 Determination. IC50's were performed in accordance with the materials and methods. IC50's were calculated using the following formula:

$$\frac{v_i}{v_o} = \frac{1}{1 + \left(\frac{[I]}{IC_{50}}\right)^h}$$

Where v_i is the initial velocity in the presence of inhibitor, v_o is the initial velocity in the absence of inhibitor, [I] is the concentration of inhibitor, IC_{50} is the concentration of inhibitor at 50% inhibition, and h is the hill slope. IC50's were determined a) for RJPXD33 (blue) and RJPXD34 (purple) against LpxD and b) for RJPXD33 (blue) against LpxA. RJPXD34 displayed no inhibition of LpxA at concentrations

up to 200 μM. Data points represent the mean of three individual experiments and error bars represent the standard deviation.

Table S1. Plasmids and bacterial strains used in this study

Bacterial strain or plasmid	Relevant characteristics	Source
Plasmids		
pACYC184	*p15A ori,* Tet^r, Cam^r	NEB
pBAD-Thio	P_{araBAD}, *trxA*, Amp^r	Invitrogen
pUC18	P_{lac}, Amp^r	Invitrogen
pBIRAcm	*birA*	Avidity
pTYB2	*intein*	NEB
pUMGD13	pTYB2::*lpxD*	This Study
pTYB2btc	pTYB2::*birA* recognition sequence	This Study
pUMRJ4	pTYB2btc::*lpxD*	This Study
pUMRJ100	*p15A ori,* P_{araBAD}, *trxA,* Cam^r	This Study
pUMRJ40	pUMRJ100::*rjpxd34-trxA*	This Study
pUMRJ41	pUMRJ100::*rjpxd33-trxA*	This Study
pUMRJ45	pUC18::*lpxD*	This Study
Strains		
E. coli		
MG1655	Wild type	ATCC
XL-1 Blue	*recA1 endA1 gyrA96 thi-1 hsdR17 supE44 relA1 lac [F′ proAB lacIqZΔM15 Tn10 (*Tet^r*)]*	Stratagene
XD33	*E. coli* XL1 Blue/pUMRJ41	This Study
XD34	*E. coli* XL1 Blue/pUMRJ40	This Study
BL21-AI	*araB::T7RNAP-tetA*	Invitrogen
JM110	*dam dcm*	Strategene

References

1. Larkin, M. A., Blackshields, G., Brown, N. P., Chenna, R., McGettigan, P. A., McWilliam, H., Valentin, F., Wallace, I. M., Wilm, A., Lopez, R., Thompson, J. D., Gibson, T. J., and Higgins, D. G. (2007) Clustal W and Clustal X version 2.0. *Bioinformatics 23*, 2947-8.